EasyChair Preprint

№ 9894

Image Fusion in SAR Images Using Fuzzy Clustering

Atul Kumar Yadav and Shubhankar Vishwakarma

March 30, 2023

Image Fusion In SAR Images Using Fuzzy Clustering

Author:-Atul Kumar Yadav And Shubhankar Vishwakarma

Abstract— ***This study provides a unique fuzzy clustering algorithm and an image fusion technique for an unsupervised distribution-free change detection method for synthetic aperture radar (SAR) images. Using complimentary data from a mean-ratio picture and a log-ratio image, the image fusion approach is introduced to create a difference image. Wavelet fusion rules based on an average operator and minimum local area energy are used to fuse the wavelet coefficients for a low-frequency band and a high-frequency band, respectively, to limit background information and increase the information of altered regions in the fused difference image. For categorizing modified and unaffected regions in the fused difference image, a reformulated fuzzy local-in-formation C-means clustering technique is suggested. Information regarding is included in it, For the objective of boosting the altered information and lessening the impact of speckle noise, spatial context is presented in an unique fuzzy manner. The image fusion technique blends the benefits of the log-ratio operator and the mean-ratio operator and improves performance, according to experiments on real SAR images. The findings of the enhanced fuzzy clustering technique for change detection showed less inaccuracy than its prior versions.***

Index Terms—**Clustering, fuzzy C-means (FCM) algorithm, image change detection, image fusion, synthetic aperture radar (SAR).**

I. Introduction

In order to find changes that may have taken place between the considered acquisition dates, image change detection is a procedure that examines photographs of the same scene obtained at several times . Due to its many uses in a variety of fields, including remote sensing , medical diagnosis , and video surveillance , it has garnered considerable interest in recent decades. Change detection in remote sensing photos is becoming increasingly and more crucial as remote sensing technology advances. Due to the existence of the speckle in synthetic aperture radar (SAR) images, change detection in SAR images presents some more challenges than optical ones. noise. SAR sensors, however, are not affected by atmospheric or lighting circumstances, which keeps the change detection in SAR images appealing .

Unsupervised change detection in SAR pictures can be broken down into three parts, as indicated in the literature: 1) image reprocessing; 2) creating a difference image between the multi-temporal images; and 3) analyzing the difference image. Noise reduction, geometric adjustments, and co registration are the key tasks of the first step. The difference image is created in the second step by pixel-by-pixel comparison of two co-registered images. Differentiating (subtraction operator) and rationing (ratio operator) are well-known methods for creating a difference image for remote sensing photos. By subtracting the intensity values between the two target images under consideration, differences between the two are measured in differentiating. In rationing, adjustments are made by using a pixel-by-pixel ratio operator on the couple under consideration. of temporal pictures. However, as the image differentiating technique is not tailored to the statistics of SAR images and is not robust to calibration errors, the ratio operator is often employed in place of the subtraction operator in the case of SAR images . Additionally, the ratio image is typically expressed in a logarithmic or a mean scale [4]-[8] due to the multiplicative nature of speckles. The histogram of the difference image is typically subjected to a judgement threshold in the third stage to identify changes. Several threshold techniques, including Otsu, the Kittler and Thrilling minimum-error threshold algorithm (K&I), and the expectation maximization (EM) algorithm, have been presented to estimate the threshold in an unsupervised way.

In general, it is evident from the literature that the effectiveness of SAR-image change detection depends heavily on the difference image's quality and the classification method's precision. In this research, we suggest an unsupervised distribution-free SAR-image change detection method to overcome the two problems. It is distinctive in the following two ways: Producing difference images by combining mean-ratio and log-ratio images, and upgrading the noise-resistant fuzzy local-information c-means (FLICM) clustering method to spot change areas without making any distribution assumptions. There are five sections in this essay. The key components of the suggested approach and our motivation will be discussed in the section that follows. The proposed method will be thoroughly explained in Section III, and experimental findings on actual multi-temporal SAR images will be discussed in Section IV to show how effective the suggested strategy is. Our conclusions are presented in the final part..

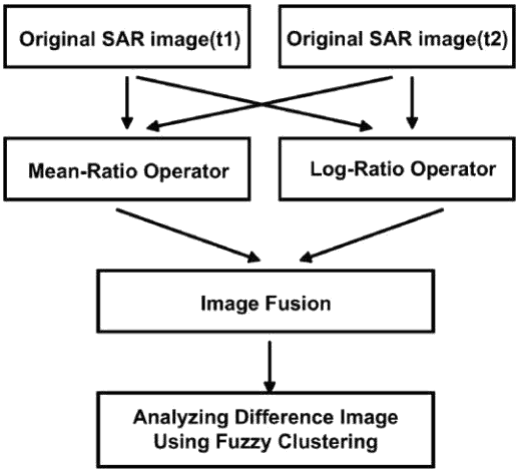

Fig. 1. Flowchart of the proposed change detection approach.

AI. Motivation

$X_1 = \{X_1(i,j), 1 < i < H, 1 < j < W\}$ and $X_2 = \{X_2(i,j), 1 < i < H, 1 < j < W\}$ $H \times W$ Let us consider the two co-registered intensity SAR images of size, i.e., ac-quired over the same geographical area at two different times t_1 and t_2, respectively. Our goal is to create a difference image that depicts the information about changes between the two points in time. A binary classification is then used to create a binary image that represents the two classes—change and unchanged. The proposed unsupervised distribution-free change detection method is divided into two phases, as depicted in Fig. 1. The mean-ratio picture and the log-ratio image are utilized to create the difference image using wavelet fusion, and the fused image is automatically analyzed using an improved fuzzy clustering technique.

Motivation of Generating Difference Images Using Image Fusion

Due to the presence of speckle noise, as was indicated in Section I, the ratio difference image is typically expressed in a logarithmic or mean scale. Since the log-normal model was regarded as a heuristic parametric probability distribution function for SAR intensity and amplitude distributions, there has been substantial worry about the ratio image's logarithm in the last 10 years . The multiplicative speckle noise can be converted into an additive noise component using the log-ratio operator. Additionally, the ratio image's range of variation will be reduced, enhancing the low-intensity pixels. In addition, the authors of proposed the ratio mean detector (RMD), which is also resistant to speckle noise. This detector anticipates that the scene will change. as a modification of the image's local mean value. Both approaches have successfully detected changes in SAR imaging, although they still have major drawbacks: The distribution of the two classes (modified and unaffected) might be made more balanced because the logarithmic scale is defined by strengthening the low-intensity pixels while weakening the pixels in the areas of high intensity. However, it's possible that the log-ratio image's information about altered regions won't be able to accurately reflect the true changes. trends in the broadest sense as a result of a weakening in the high-intensity pixel areas Because the ratio technique may highlight discrepancies in the low brightness of the temporal pictures, the background (unchanged regions) of the RMD is rather rough. The fundamental concept behind the optimal difference image is that altered areas show bigger values while untouched pixels show smaller values. That is to say, the ideal difference image should limit the information from the background (unchanged parts) and should maximize the information from the changed regions. An image fusion technique is used to construct the difference image using complimentary data from the mean-ratio image and the log-ratio in order to solve this challenge image in this paper. The information of changed regions represented by the mean-ratio picture is somewhat consistent with the true altered trends in multi-temporal SAR images, as described in the literature . On the other hand, due to the logarithmic transformation, the background information produced by the log-ratio image is comparatively flat. Consequently, it can be inferred from the research above that the new difference image created by fusing the mean-ratio image and the log-ratio image could have better information richness than the separate difference images (i.e., the mean-ratio image and the log-ratio image). Section III-A will have a thorough explanation of this method.

A. Motivation of Analyzing Difference Image Using Fuzzy Clustering

To distinguish between modified and unchanged regions, the difference image is processed. As was noted in Section I, the K&I algorithm and the EM algorithm, two common techniques for identifying the changed regions, are often carried out by applying a threshold approach to the histogram of the difference image. It is obvious that the decision threshold must be accurately estimated for this type of procedure. Additionally, they must choose an appropriate probability statistical model for the distribution of the change and unaltered classes in the difference image, which severely limits their options for use. This study proposes a novel fuzzy c-means (FCM) clustering technique to assess the difference picture, which is indifferent to the probability statistics model of histogram. In order to lessen the impact of speckle noise, this method specifically adds spatial context information into the relevant objective function. Additional information about this innovative fuzzy clustering approach is presented in Section III-B.

III. METHODS

We concentrate on describing the suggested change detection approach in this part, which consists of the following two steps:

1) Create a difference image using image fusion, and then use an upgraded FCM to find areas that have changed in the fused image.Create the Difference in A using image fusion to create

2) Image fusion describes methods that combine information from different sources to produce higher-quality data.

a number of source images such that the newly fused images are better suited to the tasks involved in computational processing. The majority of image fusion algorithms used in the last two decades operate at the pixel level of the source pictures [20]. The pixel-level image fusion has made substantial use of multi-scale transforms, particularly the discrete wavelet transform (DWT), curve lets, and contour-lets. The DWT isolates frequencies in time and space, making it simple to extract detail information from images. It has been demonstrated that transforms like curve-lets and contour lets have higher directional selectivity and properties than the DWT. However, it is clear that their computational complexity is greater than the DWT. The DWT focuses on preserving the time and frequency as well as point discontinuities.The image fusion scheme based on the wavelet transform can be described as follows: First, we compute the DWT of each of the two source images and obtain the multi resolution commode position of each source image. Then, we fuse corresponding coefficients of the approximate and detail sub-bands of the de composed source images using the developed fusion rule in the wavelet-transform domain. In particular, the wavelet coefficients are fused using different fusion rules for a low-frequency band and a high-frequency band, respectively. Finally, the in verse DWT is applied to the fused multi resolution representation to obtain the fused result image.

The following is a description of the wavelet-based picture fusion method: To begin, we determine the DWT of each of obtain the multi-resolution decomposition of each of the two source images. Then, using the created fusion rule in the wavelet-transform domain, we combine the appropriate coefficients of the approximate and detail sub-bands of the decomposed source images. In particular, for a low-frequency band and a high-frequency band, respectively, the wavelet coefficients are fused using various fusion algorithms. The fused result image is then created by applying the-inverse DWT to the multi resolution representation that has been combined.

The mean-ratio picture and the log-ratio image, respectively, are represented here as and. H and L stand for high-pass respectively, high-pass and low-pass filters. Additionally, LH, HL, and HH stand for the portions of the image that are in the horizontal, vertical, and diagonal directions, respectively. LL stands for the approximate portion of the image. represents the merged image.Each source image is decomposed into four identical images after one degree of decomposition, as seen in Fig. 2. The approximation section of the low-frequency sub-band, which is what it is termed, represents the source image's profile traits. Three high-frequency sub-bands, and, which represent the parts in the horizontal, vertical, and diagonal directions, respectively, display the details of the key edges and lines in the original image.

From the approximate (low-frequency sub-band) and detail, it can be concluded that the approximate coefficients of the decomposition level can be determined (high-frequency sub-bands)factors at the level. Additionally, because the low-frequency sub-band and the high-frequency sub-band reflect various feature information of the source images, it is important to fuse the wavelet coefficients using various fusion algorithms.

The selection of fusion rules, which should limit background (unchanged areas) information and should increase the information of changed regions, is the main challenge of the suggested approach to generate difference image. In the last two decades, a wide variety of fusion rules have been put forth in the literature to obtain the fused coefficient, including the rule of selecting the coefficients from local features like maximum variance or contrast, or the rule of selecting the coefficients with the highest absolute value of the corresponding wavelet coefficients.However, the changed and unchanged classes should be fused in different schemes, meaning that the background should be inhibited from the viewpoint of the ideal difference image.

By simply enhancing the gradient or edge features of the fused image, the background information in the difference image may become rough. Therefore, it is essential to create an adaptive strategy for the fusing of source images that may limit background information and maximize the enhancement of information for altered regions.

Here, the minimum local area energy coefficient and the rule of choosing the average value of the corresponding coefficients for the low-frequency band are both used.For the low-frequency sub band, the wavelet coefficients are fused using the rule of the average operator. On the other hand, the rule of lowest local area energy of wavelet coefficients is chosen to suppress the background clutter for high-frequency sub bands that reveal information about the important elements of the source image, such as edges and lines. This rule aims to merge the homogeneous portions of the mean-ratio picture and the log-ratio image's high-frequency portion. The adoption of high frequency from the log-ratio picture will somewhat suppress the background in the new fused difference image since the background of the log-ratio image is relatively flat (see Section II).It should be mentioned that the multi-resolution decomposition process is used to carry out the suggested strategy to generate the difference image.

Since the histogram of the fused difference picture comprises both the log-ratio image information and the mean-ratio image information at various resolution levels, the probability statistics model for the histogram may be challenging. Because both K&I and EM presume that the histogram of the difference picture corresponds to a specific probability statistics model, they may not be suitable for use in analyzing the fused difference image. As can be observed from the analysis above, in order to analyse the fused data, a classification approach that is insensitive to the probability statistics model of histogram is necessary.To assess the difference image produced by the wavelet fusion, we therefore suggested an unique FCM clustering approach in the next section.The goal of processing the difference image is to distinguish between changed and unaltered areas. Additionally, clustering is a classification method that groups items or patterns so that samples from the same cluster have a higher degree of similarity than samples from other clusters. As a result, it is possible to think of the challenge of change detection as a clustering problem where the key is to categorize the different image data into two groups.

Additionally, the statistical model for change and unaltered class distributions has no bearing on the clustering technique, opening up a wide range of possibilities for SAR-image change detection. The FCM algorithm is one of the most well-liked clustering techniques since it can preserve.

Provides additional details from the source image and has strong ambiguity qualities.The conventional FCM algorithm, however, is extremely susceptible to noise because it ignores any spatial context information.

To address this shortcoming of FCM, numerous researchers have recently added local spatial and local gray-level information to the original FCM algorithm .The FCM S that Ahmed suggested modifies the classical FCM's objective function to account for intensity in homogeneity and to permit the labeling of a pixel to be influenced by labels dis its immediate vicinity. However, because it computes the neighbourhood term at each iteration step, FCM S has a much higher computational complexity than the original FCM.The fast generalized FCM (FGFCM) algorithm was developed by Caietal to speed up the processing of the FCM S algorithm. By clustering on the gray-level histogram rather than on pixels, it can significantly reduce execution time while also being somewhat less sensitive to noise due to the addition of local spatial information. However, both of them have the following shortcomings when it comes to the unsupervised SAR-image change detection task: In order to strike a compromise between resilience to noise and efficacy of preserving the features of the image, an artificial parameter is employed in their objective functions.Since there is no prior knowledge of the speckle noise level, the parameter selection is not simple to implement.The choice of the parameter must typically be made by trial and error or through experience. A robust FLICM clustering technique has recently been presented by Krindis and Chatzisto address the aforementioned flaw. Let's now concentrate on this algorithm's analysis and present our improvement.

First, the FLICM Clustering Algorithm The use of a fuzzy local similarity measure, which aims to ensure noise insensitivity and image detail retention, is a distinguishing feature of FLICM. To improve the clustering efficiency, a novel fuzzy factor is added to the FLICM's object function. The spatial Euclidean distance between pixels and is where the pixel indicates the nearby pixels falling into the window around the pixel and the th pixel represents the centre of the local window. reflects the fuzzy membership of the grey value with respect to the cluster as well as the prototype of the cluster's centre.

As can be observed, the trade off between picture noise and image features is controlled by the factor without any artificial parameters being set. Additionally, the spatial Euclidean distance of pixels within the local window from the centre pixel is used to control the influence of those pixels in a flexible manner. Therefore, the spatial distances from the core pixel can reflect the damping extent of the neighbour with various spatial positions or separations from the primary pixel. The corresponding membership values of the no-noisy pixels as well as the noisy pixels that are falling into the local window will typically change with the application of the fuzzy factor.converge to a comparable value, balancing the membership values of the window's pixel locations. FLICM becomes more resistant to outliers as a result. In addition, Flick's attributes include immunity to noise, preservation of image details without the use of artificial parameters, and direct application to the original image.

The objective function of the FLICM can be described in terms of by utilizing the definition of where is the number of data items, is the number of clusters, represents the prototype value of the cluster, and represents the fuzzy membership of the pixel with respect to the cluster. is an object's distance in Euclidean space from the cluster's centre.

Additionally, the following procedure is used to calculate the cluster centers and the membership partition matrix:- FLICM modification: It can be deduced from the study of the fuzzy factor that the local gray-level information and spatial information are represented, respectively, by the gray-level difference and the spatial distance. Additionally, depending on spatial distances from the central pixel, the local spatial connection adapts. The spatial distances from the central pixel are used by the authors of FLICM to calculate the damping extent of the neighbour. The damping extent decreases with increasing spatial distance for neighbouring pixels with the same gray-level value, and vice versa. However, in some circumstances, the spatial distance utilize to calculate the neighbour damping extent may be arbitrary. Here are two instances in two different scenarios.

A120	22	13
32	20	35
28	B90	27

(a)

87	99	116
90	20	67
110	88	75

(b)

0.414	0.5	0.414
0.5		0.5
0.414	**0.5**	0.414

(c)

Case 1) The central pixel is not noise, and some pixels within its local window may be corrupted by noise. A 3
3 window. That is extracted from the noise image depicts this situation, and
picts its damping extent of the neighbors with the spatial distances . In this case, the gray values of the noisy pixels are far different from the other pixels within the window. For the noisy pixels of A and B, the gray-level difference between pixel A and the central pixel is greater than pixel B. In order to suppress the influence of the noisy pixels as far as possible, the weightings added of pixel A in should be able to reflect a stronger trend in contrast with the noisy pixel B. However, the damping extent of the neighbors with the spatial distances shows the opposite trend.

Case 2) The central pixel is corrupted by noise, whereas the other pixels within its local window are homage
nous and not corrupted by noise. An example that illustrates this situation is demonstrated.In this case, the gray-level differences between the neighboring pixels and the central pixel are some
what different. To estimate the fuzzy factor rigorously, the damping extent of the neighboring pixels is supposed to be treated separately. However,the damping extent of the neighbors that is reflected by the spatial distances is simply

divided into two categories (0.414 and 0.5). It fails to analyze exhaustively the

impact of each neighboring pixel onto the fuzzy factor .The foregoing analysis highlights the importance of the ac
curate estimation of the fuzzy factor to suppress effectively the influence of the noisy pixels. In order to overcome the short coming mentioned above, in this paper, the local coefficient of variation is adopted to replace the spatial distance.The analysis presented above emphasizes how crucial it is to estimate the fuzzy factor accurately in order to successfully reduce the influence of noisy pixels. The local coefficient of variation is used in place of the spatial distance in this work to address the aforementioned flaw. Additionally, the intensity variance and mean in a local window of the image, respectively, are and the local coefficient of variation is defined by var.

The value of represents the local window's degree of gray-value homogeneity. It displays high values at the margins or in the noise-damaged area and generates low values in homogeneous areas. The area-type of analysis is used to determine the damping extent of the neighbors with local coefficient of variation.They will have extremely similar local coefficient of variation results, and vice versa. In general, the difference in the local coefficient of variation between adjacent pixels and the centre pixel is rather consistent with the spatial distance.Since each pixel's local coefficient of variation is calculated in a local window, additional local context information can be utilize.

Since each pixel's local coefficient of variation is calculated in a local window, additional local context information can be utilize.

The modified fuzzy factor in this case can be described as follows: If the local coefficient of variation of the central pixel, denotes the local coefficient of variation of surrounding pixels, and is the mean value that is situated in a local window. The reformulated factor, as seen in (11), balances the membership value of the central pixel while taking into account the local coefficient of variation and the Grey level of the surrounding pixels. If there is a clear distinction between the local coefficient of variation results acquired by the central and nearby pixels.

IV. EXPERIMENTAL STUDY

In this section, we will demonstrate the performance of the suggested approaches by showing numerical results on three data sets in order to validate the efficacy of the proposed SAR-image change detection method. The first data set is a segment (301 301 pixels) of two SAR images taken in April and May 1999 over a region close to Bern, Switzerland, using the European Remote Sensing 2 satellite's SAR sensor. Parts of the cities of Thun and Bern, as well as the airport in Bern, were completely inundated by the River are between the two dates. Therefore, a test site for identifying floodplains was chosen in the are Valley between Bern and Thun. The reference image, which represented the available ground truth,\The second data set consists of a portion (290 350 pixels) of two SAR images taken by the Radarsat above the city of Ottawa. SAR detector. They came from Ottawa, Canada's Defense Research and Development Canada. The automatic registration algorithm from A.U.G. Signals Ltd., which is accessible through distributed computing at www.signalfusion.com, was used to register these photos.

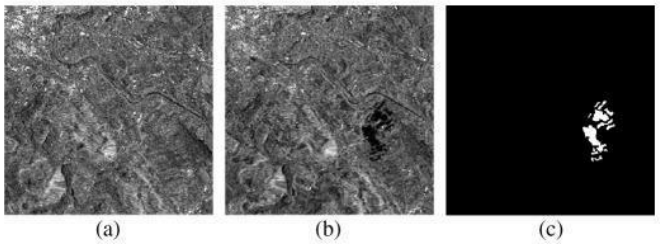

Multi-temporal images relating to the city of Bern used in the experiments. (a) Image acquired in April 1999 before the flooding. (b) Image acquired in May 1999 after the flooding. (c) Ground truth.

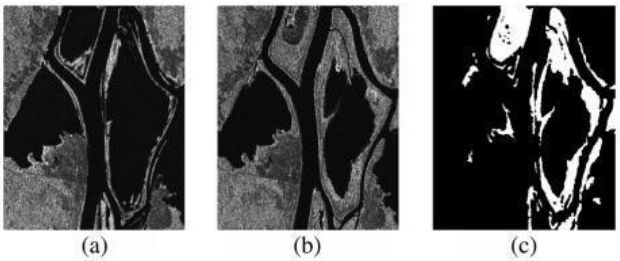

Multi temporal images relating to Ottawa used in the experiments. (a) Image acquired in July 1997 during the summer flooding. (b) Image acquired in August 1997 after the summer flooding. (c) Ground truth.

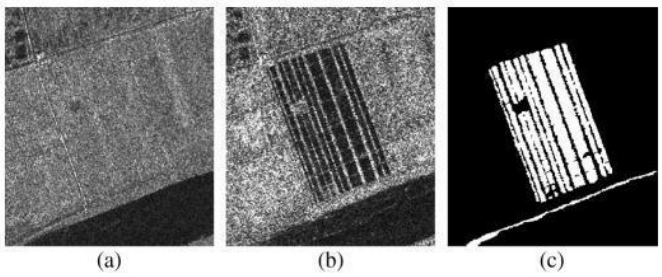

Multi temporal images relating to the Yellow River Estuary used in the experiments. (a) Image acquired in June 2008. (b) Image acquired in June 2009 (c) Ground truth.these pictures—water and land. The reference image (ground truth) depicted in (c) was produced by combining prior knowledge with photo interpretation based on the input photos in Fig (b).Two SAR photos taken by Radarsat-2 in June 2008 and June 2009 at the Yellow River Estuary in China made up the third data set used in the trials. These two SAR photos were captured by Radarsat-2, and their original size is 7666 7692. To display the detail information in such little pages, they are excessively large. We choose a restricted area with a size of 257 289 pixels to compare the results of the change detection techniques. The truth as it currently stands (reference image).Based on the input photos in Fig.(a) and other sources, information with

photo interpretation (b). It should be highlighted that the two photos under consideration are, respectively, single-look and four-look images.

This indicates that the impact of speckle noise on the 2009 image is significantly bigger than the 2008 image. The processing of change detection may become more challenging due to the significant variance in speckle noise levels between the two images used.There have been two experiments run, each with a distinct goal. The first experiment is to evaluate the wavelet fusion strategy's efficacy in producing the difference image. Additionally, we contrasted our algorithm's ability to detect changes with that of the mean-ratio operator and the log-ratio operator. To calculate the local area energy of the wavelet coefficient, a 3 3 sliding window is chosen. In particular, the outcomes of the change detection achieved by the aforementioned difference images are assessed using two straightforward classification algorithms, namely K-means and Otsu. In the second experiment, we examined how the RFLICM method affected the outcomes of the fused difference image's change detection.The results of the quantitative analysis of change detection are as follows. First, we determine the negative errors (FN, changed pixels that undetected). Second, we determine the false positives (FPs), or unmodified pixels that were incorrectly classified as changed.

Third, we estimate the fraction of correctly classified data (PCC). Given by PCC, TP, TN, TP, FP, and FN (12)

TP stands for true positives in this context, which is the quantity of pixels that are identified as the altered region in both the reference image and the outcome. The term "true negatives" refers to the number of pixels that are identified as the same area in both the reference image and the final image.In the first experiment, we evaluated the wavelet image fusion technique's efficacy in producing the difference image. The distinct images produced by the three various

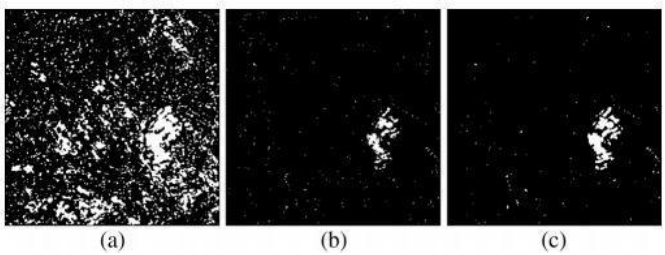

(a) (b) (c)

In next figure, various techniques (mean-ratio, log-ratio, and wavelet fusion) are displayed. The merged difference image [see Fig.(c)] gives off an evocative gut reaction. The step variations [6] are in accordance. Change detection results of the Bern data set based on the three difference images obtained by Otsu. (a) Based on the mean-ratio operator.

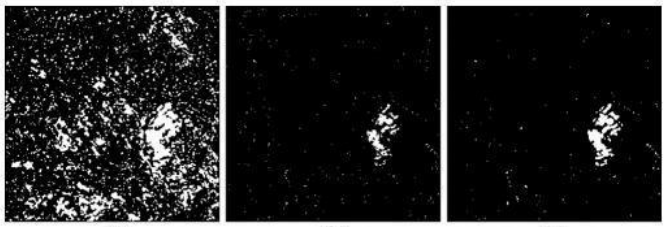

(a) (b) (c)

Change detection results of the Bern data set based on the three difference images obtained by K-means. (a) Based on the mean-ratio operator. (b)

Based on the log-ratio operator. (c) Based on wavelet fusion to a strong modification of the land cover that occurred between two images is well reflected, and then the background(unchanged regions) in fused image is inhibited to a certain degree with the use of wavelet coefficients of log-ratio image.As shown in Tables I and II, the change detection results of the fused difference image were compared with the ones generate from mean-ratio operator and log-ratio operator by Otsu and K-means, respectively. It can be seen from the analysis of the PCC that, the change detection results of mean-ratio difference image that achieved by both methods was disastrous. For the log-ratio operator, the PCC yielded was equal to 99.27% for Otsu, and 99.24% for K-means. And the proposed approach resulted in the highest PCC (99.35% for Otsu and 99.36% for K-means) and kappa (0.781 for Otsu and 0.784 for K-means).

By a visual analysis of Figs. 8 and 9, we can have a better understanding of the behavior of the three different methods.

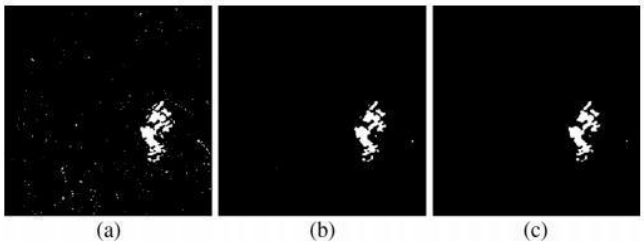

(a) (b) (c)

Change detection results of the Bern data set achieved by (a) FCM,(b) FLICM, and (c) proposed RFLICM.(a) and 9(a) depict the change detection results obtained from the mean-ratio image, which reveal that it has more spots than the other two methods because of the effect of the speckle phenomenon. As can be seen from Figs. 8(b) and 9(b), the change detection maps obtained from the log-ratio image have lesser spots because of the logarithmic transformation. However, it also caused the loss of information in changed areas since the operation of log-ratio may abate the labour-intensive. The change detection maps yield from the wavelet fusion image are shown in the above both figure.As can be concluded from above analysis, the method that we proposed can effectively reduce the errors in the change detection results.SAR-image change detection which based on the wavelet fusion difference image, in the second experiment, a comparison was carried out among traditional FCM, FLICM and RFLICM.

According to Fig.shown(a), the change detection map achieved by

traditional FCM contains lots of spots. This is explained by the fact that it fail to consider any information about spatial context. By contrast, by incorporating the local information, the change detection maps generated by FLICM [Fig. 10(b)] and RFLICM [Fig. shown(c)] were robust to the outliers. As shown in Table III, it depicts the behavior of kappa, PCC, FP and FN among these three methods. The PCC yielded by RFLICM, FLICM and FCM were equal to 99.68%, 99.66% and 99.37%, respectively. RFLICM outperforms FLICM and FCM obviously.B. Results on the Ottawa Data Set The first experiment is aimed at analyzing the effectiveness.of the proposed approach that is based on the wavelet fusion.
Fig. Shown represents the difference images generated by the mean ratio, the log ratio, and the wavelet fusion. The change detection results generated from the three difference images have been shown in Figs. 12 and 13. In particular, as shown in Figs.(a), due to the reason of image speckle noise, the change detection maps generated from the mean-ratio difference image swarmed with isolated spots, whether using Otsu or K-means.

As for the log-ratio difference image, the change detection maps.

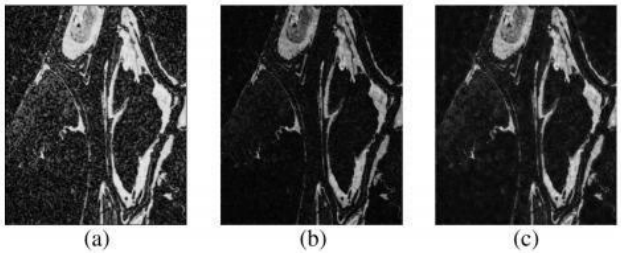

(a) (b) (c)

Fig. 12. Change detection results of the Ottawa data set based on the three
difference images obtained by Otsu. (a) Based on the mean-

ratio operator.(b) Based on the log-ratio operator. (c) Based on wavelet fusion.Fig. 13. Change detection results of the Ottawa data set based on the three difference images obtained by K-means. (a) Based on the mean-ratio operator.(b) Based on the log-ratio operator. (c) Based on wavelet fusion.
are illustrated in Figs. 12(b) and 13(b). The problem of losing information in change regions persists, with the fact that the missed alarms caused by Otsu and K-means were up to 1942 pixels and 1926 pixels, respectively. Conversely, the change detection maps achieved from wavelet fusion [see Figs. 12(c) and 13(c)] are very close to the ground-truth map illustrated in Fig. 5(c). As reported in Tables IV and V, the maximum PCC and kappa are achieved by the fused difference image.
In the second experiment, to assess the suitability of the presented RFLICM algorithm for the wavelet fusion difference image, a comparison analysis was carried out on two other methods (FCM and FLICM). Change detection maps obtained by FCM, which is sensitive to noise [illustrated in Fig. 14(a)], confirm the necessity of incorporating the information about spatial context. As reported in Table VI, the proposed RFLICM
resulted in the highest PCC and kappa. The quantitative anal sis confirm the suitability of the RFLICM algorithm on the fused difference image.

C. Results on the Yellow River Estuary Data Set
Unlike the Bern or Ottawa data sets, the influence of speckle noise on the image acquired in 2009 is much greater than the one acquired in 2008 since the two images considered are a single-look image and a four-look image, respectively. It rep resents a more complicated situation to assess the effectiveness of the proposed approach. Fig. 15 represents the difference images generated by the mean ratio, the log ratio, and the wavelet

fusion. The change detection maps achieved by FLICM and RFLICM are illustrated in Figs. 16 and 17, respectively.
As shown in Figs. 16 and 17, lots of spots are contained in the changed detection map that is generated from the mean-ratio operator [see Figs. 16(a) and 17(a)]. On the other hand, for the change detection maps generated from the log ratio [see Figs. 16(b) and 17(b)], too much information has been lost, although it exhibits less spots. By comparison, the difference image generated by wavelet fusion can reflect the real change trend as well as mitigate the impact of speckle noise [see Figs. 16(c) and 17(c)]. Moreover, as reported in Tables VII and
VIII, the fused difference image resulted in the highest PCC and kappa.

The visual and quantitative results on the Yellow River es teary data set confirm the suitability of the RFLICM algorithm on the fused difference image. As a matter of fact, RFLICM and
FLICM incorporate both local spatial and gray information to find a trade-off between detail preservation and noise removal. The proposed RFLICM attends to evaluate the local information more precisely than FLICM.

V. CONCLUDING REMARKS

In this paper, we have presented a novel SAR-image change detection approach based on image fusion and an improved fuzzy clustering algorithm, which is quite different from the existing methods. First, for the wavelet fusion approach that we proposed, the key idea is to restrain the background (unchanged areas) information and to enhance the information of changed regions in the greatest extent. As mentioned in the literature, the information of changed regions reflected by the mean-ratio image is relative in accordance with the real changed trends in multi temporal SAR images. On the other hand, the information of background obtained by the log-ratio image is relatively flat on account of the logarithmic transformation. Hence, complementary information from the mean-ratio image and the
log-ratio image is utilized to fuse a new difference image. Com

pared with other existing methods (mean ratio and log ratio),

the proposed approach can reflect the real change trend as well as restrain the background (unchanged areas). Second, in contrast with the log-ratio image and the mean-ratio image, the estimation of the probability statistics model for the histogram of the fused difference image may be complicated since it incorporates both the log-ratio and mean-ratio image information at different resolution levels. Hence, the threshold technique, such as K&I and EM, may be un-adapted to analyze the fused difference image since both of them assume the histogram of the difference image corresponding to the certain probability statistics model. Here, the RFLICM algorithm that incorporates both local spatial and gray information is proposed, which is relatively insensitive to probability statistics model. The RFLICM algorithm introduces the reformulated factor as a local similarity measure to make a trade-off between image detail and noise. Compared with the original algorithms, RFLICM is able to incorporate the local information more exactly. The experiment results show that the proposed wavelet fusion strategy can integrate the advantages of the log-ratio operator and the mean-ratio operator and gain a better performance.

The change detection results obtained by the RFLICM exhibited less spots than its preexistence (i.e., FLICM) since it is able to incorporate the local information more exactly

ACKNOWLEDGMENT

The authors would like to thank Dr. Krinidis for providing their FLICM source codes for comparisons and the editors and anonymous reviewers for their valuable comments and helpful suggestions, which greatly improved the quality of this paper.

REFERENCES

[1] R. J. Radke, S. Andra, O. Al-Kofahi, and B. Roysam, "Image change detection algorithms: A systematic survey," IEEE Trans. Image Process., vol. 14, no. 3, pp. 294–307, Mar. 2005.

[2] L. Bruzzone and D. F. Prieto, "An adaptive semiparametric and context-based approach to unsupervised change detection in multi-temporal remote-sensing images," IEEE Trans. Image Process., vol. 11, no. 4, pp. 452–466, Apr. 2002.

[3] A. A. Nielsen, "The regularized iteratively reweighed MAD method for change detection in multi- and hyper spectral data," IEEE Trans. Image Process., vol. 16, no. 2, pp. 463–478, Feb. 2007.

[4] Y. Bazi, L. Bruzzone, and F. Melgani, "An unsupervised approach based on the generalized Gaussian model to automatic change detection in multitemporal SAR images," IEEE Trans. Geosci. Remote Sens., vol. 43, no. 4, pp. 874–887, Apr. 2005.

[5] F. Bovolo and L. Bruzzone, "A detail-preserving scale-driven approach to change detection in multitemporal SAR images," IEEE Trans. Geosci. Remote Sens., vol. 43, no. 12, pp. 2963–2972, Dec. 2005.

[6] F. Bujor, E. Trouvé, L. Valet, J. M. Nicolas, and J. P. Rudant, "Application of log-cumulants to the detection of spatiotemporal discontinuities in multitemporal SAR images," IEEE Trans. Geosci. Remote Sens., vol. 42, no. 10, pp. 2073– 2084, Oct. 2004.

[7] F. Chatelain, J.-Y. Tourneret, and J. Inglada, "Change detection in multisensor SAR images using bivariate Gamma distributions," IEEE Trans. Image Process., vol. 17, no. 3, pp. 249–258, Mar. 2008.

[8] J. Inglada and G. Mercier, "A new statistical similarity measure for change detection in multitemporal SAR images and its extension to multiscale change analysis," IEEE Trans. Geosci. Remote Sens., vol. 45, no. 5, pp. 1432–1445, May 2007.

[9] S. Marchesi, F. Bovolo, and L. Bruzzone, "A context-sensitive technique robust to registration noise for change detection in VHR multispectral images," IEEE Trans. Image Process., vol. 19, no. 7, pp. 1877–1889, Jul. 2010.

[10] A. Robin, L. Moisan, and S. Le Hegarat-Mascle, "An a-contrario approach for subpixel change detection in satellite imagery," IEEE Trans. Pattern Anal. Mach. Intell., vol. 32, no. 11, pp. 1977–1993, Nov. 2010.

[11] M. Bosc, F. Heitz, J. P. Armspach, I. Namer, D. Gounot, and L. Rum
bach, "Automatic change detection in multimodal serial MRI: Application to multiple sclerosis lesion evolution," Neuroimage, vol. 20, no. 2, pp. 643–656, Oct. 2003.

[12] D. Rey, G. Subsol, H. Delingette, and N. Ayache, "Automatic detection and segmentation of evolving processes in 3-D medical images: Application to multiple sclerosis," Med. Image Anal., vol. 6, no. 2, pp. 163–179, Jun. 2002.

[13] D. M. Tsai and S. C. Lai, "Independent component analysis-based background subtraction for indoor surveillance," IEEE Trans. Image Process., vol. 18, no. 1, pp. 158–167, Jan. 2009.

[14] S. S. Ho and H. Wechsler, "A martingale framework for detecting changes in data streams by testing exchangeability," IEEE Trans. Pattern Anal. Mach. Intell., vol. 32, no. 12, pp. 2113–2127, Dec. 2010.

[15] A. Singh, "Digital change detection techniques using remotely sensed data," Int. J. Remote Sens., vol. 10, no. 6, pp. 989–1003, 1989.

[16] E. J. M. Rignot and J. J. Van Zyl, "Change detection techniques for ERS-1 SAR data," IEEE Trans. Geosci. Remote Sens., vol. 31, no. 4, pp. 896–906, Jul. 1993.

[17] M. Sezgin and B. Sankur, "A survey over image thresholding techniques and quantitative performance evaluation," J. Electron. Imag., vol. 13, no. 1, pp. 146–165, Jan. 2004.

[18] S. Krinidis and V. Chatzis, "A robust fuzzy local information C-means clustering algorithm," IEEE Trans. Image Process., vol. 19, no. 5, pp. 1328–1337, May 2010.

[19] E. E. Kuruoglu and J. Zerubia, "Modeling SAR images with a generalization of the Rayleigh distribution," IEEE Trans. Image Process., vol.13, no. 4, pp. 527–533, Apr. 2004.

[20] G. Piella, "A general framework for multiresolution image fusion: From pixels to regions," Inf. Fusion, vol. 4, no. 4, pp. 259–280, Dec. 2003.

[21] J. C. Bezdek, Pattern Recognition With Fuzzy Objective Function.

[22] M. Ahmed, S. Yamany, N. Mohamed, A. Farag, and T. Moriarty, "A modifified fuzzy C-means algorithm for bias fifield estimation and segmentation of MRI data," IEEE Trans. Med. Imag., vol. 21, no. 3, pp. 193–199, Mar. 2002.

[23] W. Cai, S. Chen, and D. Zhang, "Fast and robust fuzzy C-means clustering algorithms incorporating local information

for image segmentation," Pattern Recognit., vol. 40, no. 3, pp. 825–838, Mar. 2007.
[24] P. L. Rosin and E. Ioannidis, "Evaluation of global image thresholding for change detection," Pattern Recognit. Lett., vol. 24, no. 14, pp. 2345–2356, Oct. 2003.
[25] G. H. Rosenfifield and A. Fitzpatrick-Lins, "A coeffificient of agreement as a measure of thematic classifification accuracy," Photogramm. Eng. Remote Sens., vol. 52, no. 2, pp. 223–227, 1986.

Maoguo Gong (M'07) received the B.Eng. degree in electronic engineering (with fifirst class honors) and Ph.D. degree in electronic science and technology from Xidian University, Xi'an, China, in 2003 and 2009, respectively. Since 2006, he has been a Teacher with Xidian University. In 2008 and 2010, he was promoted as an Associate Professor and as a Full Professor, respectively, both with exceptive admission. He is currently a Full Professor with the Key Laboratory of Intelligent Perception and Image Understanding of the Ministry of Education, Xidian University. His research interests include computational intelligence with applications. His current research interests include change detection in remote sensing and medical images. Dr. Gong is a member of the IEEE Computational Intelligence Society, an Executive Committee Member of the Natural Computation Society of Chinese Association for Artifificial Intelligence, and a Senior Member of the Chinese Computer Federation. He was the recipient of the New Century Excellent Talent in University of the Ministry of Education of China, the Eighth Young Scientist Award of Shaanxi, the New Scientifific and Technological Star of Shaanxi Province, the Excellent Yong Contributor of Shaanxi Province, the Elsevier Scopus Young Scientist Award in Sustainable Development of China, and the Science and Technology Award of Shaanxi Province (First Level, 2008 and 2010), etc.

Zhiqiang Zhou received the B.S. degree in electronic engineering from Xidian University, Xi'an, China, in 2009, where he is currently working toward the M.S. degree. His research interests include change detection in remote sensing images.

Jingjing Ma received the B.S. degree in electronic engineering from Xidian University, Xi'an, China, in 2004, where he is currently working toward the Ph.D. degree. Her current research interests include computational intelligence and image understanding.